Molecular Therapy
Methods & Clinical Development
Original Article

Human Umbilical Tissue-Derived Cells Secrete Soluble VEGFR1 and Inhibit Choroidal Neovascularization

Jing Cao,[1] Rong Yang,[2] Taylor E. Smith,[2] Stephanie Evans,[2] Gary W. McCollum,[2] Steven C. Pomerantz,[1] Theodore Petley,[1] Ian R. Harris,[1] and John S. Penn[2]

[1]Janssen Research & Development, LLC, Spring House, PA 19477, USA; [2]Department of Ophthalmology and Visual Sciences, Vanderbilt University School of Medicine, Nashville, TN 37232, USA

Exudative age-related macular degeneration (AMD), characterized by choroidal neovascularization (CNV), is the leading cause of irreversible blindness in developed countries. Anti-vascular endothelial growth factor (VEGF) drugs are the standard treatment for AMD, but they have limitations. Cell therapy is a promising approach for ocular diseases, and it is being developed in the clinic for the treatment of retinal degeneration, including AMD. We previously showed that subretinal injection of human umbilical tissue-derived cells (hUTCs) in a rodent model of retinal degeneration preserved photoreceptors and visual function through rescue of retinal pigment epithelial (RPE) cell phagocytosis. Here we investigated the effect of hUTCs on a rat model of laser-induced CNV and on a human RPE cell line, ARPE-19, for VEGF production. We demonstrate that subretinal injection of hUTCs significantly inhibited CNV and lowered choroidal VEGF *in vivo*. VEGF release from ARPE-19 decreased when co-cultured with hUTCs. Soluble VEGF receptor 1 (sVEGFR1) is identified as the only factor in hUTC conditioned medium (CM) that binds to VEGF. The level of exogenous recombinant VEGF in hUTC CM was dramatically reduced and could be recovered with sVEGFR1-neutralizing antibody. This suggests that hUTC inhibits angiogenesis through the secretion of sVEGFR1 and could serve as a novel treatment for angiogenic ocular diseases, including AMD.

INTRODUCTION

Age-related macular degeneration (AMD) is the main cause of visual impairment and blindness in people aged over 65 years in developed countries. There are two forms of AMD, dry (atrophic) and wet (exudative). Wet AMD is characterized by the formation of choroidal neovascularization (CNV) that leads to the deterioration of central vision and irreversible visual impairment.[1] About 85% of patients with AMD have the dry form, while about 15% of patients progress to the wet or neovascular form of AMD.[1,2] Vascular endothelial growth factor (VEGF) is the crucial regulator of angiogenesis, and it plays a critical role in the formation of neovascularization in wet AMD.[3,4] Evidence suggests that retinal pigment epithelial (RPE) cells are an important source of VEGF in wet AMD, contributing to CNV formation.[5–7] VEGF is overexpressed in the RPE of autopsy eyes with AMD and in RPE cells of surgically excised CNV membranes.[8–11] Factors implicated in AMD, such as complement activators and reactive oxygen intermediates, are potent stimuli of VEGF expression in RPE cells.[6,12,13] Additionally, in animal studies, overexpression of VEGF in the RPE can lead to CNV.[14–16]

VEGF mediates its angiogenic effects by binding to specific VEGF receptors. Of the primary receptors, VEGFR1 and VEGFR2 are mainly associated with angiogenesis, whereas VEGFR3 is associated with lymphangiogenesis.[17] The soluble form of VEGFR1 results from alternative splicing of VEGFR1, and it is a naturally occurring endogenous inhibitor of VEGF that acts by sequestering VEGF from signaling receptors and forming non-signaling heterodimers with VEGFR2.[18] Currently, anti-VEGF drugs are the standard treatment for this condition, but they must be repeatedly administered over a long period of time, placing a burden on patients and often leading to undertreatment and subsequent vision loss.[19–21]

Recently, efforts have been made to develop cell-based therapies for the treatment of retinal diseases, including AMD.[22,23] Administration of human umbilical tissue-derived cells (hUTCs) is being developed as a novel cell therapy for the treatment of geographic atrophy (GA), the advanced dry form of AMD.[24] Because AMD patients typically develop the dry form first, while wet AMD typically occurs on a background of dry AMD, dry AMD is often considered a precursor state for wet AMD.[25,26] Indeed, GA represents the greatest risk factor for advancing to wet AMD. Neovascular lesions are often present in the periphery of eyes with GA.[27,28]

To date, the effect of hUTCs on neovascularization in the eye is unknown. Hence, we examined the effect of hUTCs in the laser-induced

Received 10 September 2018; accepted 10 May 2019;
https://doi.org/10.1016/j.omtm.2019.05.007.

Correspondence: Jing Cao, MD, PhD, Oncology Translational Research, Janssen Research & Development, LLC, Spring House, PA 19477, USA.
E-mail: jcao5@its.jnj.com
Correspondence: John S. Penn, PhD, Department of Ophthalmology and Visual Sciences, Vanderbilt University School of Medicine, Nashville, TN 37232, USA.
E-mail: john.penn@vanderbilt.edu

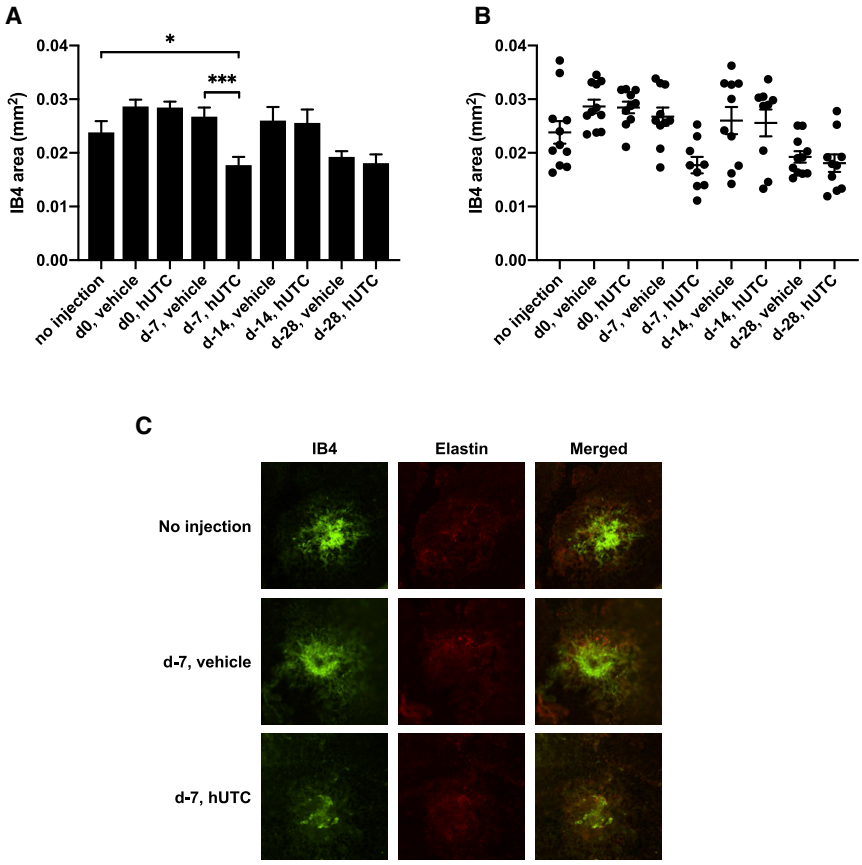

Figure 1. hUTCs Inhibited Choroidal Neovascularization *In Vivo*

(A and B) Rats were treated with subretinal injections of vehicle or hUTCs at 0, 7, 14, or 28 days prior to laser application or assigned to a no-injection control group. All rats were sacrificed 14 days after laser application. Areas of IB4-stained lesions were measured. Lesion sizes were measured from between 9 and 11 retinas for each treatment group. Lesion size was significantly decreased with hUTC injection 7 days prior to laser application (day 7) when compared to the day 7 vehicle control ($p = 0.0007$) and when compared to the no-injection group ($p = 0.0178$). Data represent mean ± SEM. (C) IB4 and elastin stainings of representative lesions show the decreased lesion size associated with hUTC injections when compared to the no-injection and vehicle control groups. Data represent mean ± SEM in bar graph (A) and scatter plot (B) format. *$p < 0.05$, ***$p < 0.001$.

rodent model of CNV and on RPE VEGF production. Herein, we demonstrate that hUTCs significantly inhibited CNV and reduced choroidal VEGF *in vivo*. Also, VEGF release from ARPE-19 was dose-dependently decreased when the cells were co-cultured with density-dependent hUTCs. Soluble VEGF receptor 1 (sVEGFR1) was detected in the conditioned medium (CM) of hUTCs, and it is shown to be the only factor in the CM that bound VEGF, as analyzed by immunoprecipitation and mass spectrometry (MS). The level of recombinant human VEGF was dramatically reduced in hUTC CM, and it could be recovered by a neutralizing antibody against sVEGFR1. These results suggest that hUTCs have the potential to inhibit VEGF-induced angiogenesis through the secretion of sVEGFR1 and may be developed as a novel cell therapy for the treatment of angiogenic ocular diseases.

RESULTS

Efficacy of hUTCs in the Rat LCNV Model

Laser-induced CNV (LCNV) rats received subretinal injections of hUTCs or vehicle at 28, 14, 7, or 0 days pre-laser treatment. LCNV lesion size was assessed 14 days post-laser treatment. We found a significant difference between the 7-day pre-laser vehicle and hUTC groups; the mean ± SEM (mm^2) values were 0.026761 ± 0.00177 mm^2 and 0.017721 ± 0.00187 mm^2 ($p = 0.0007$), respectively, corresponding to a 34% reduction in LCNV (Figures 1A and 1B). A significant difference was also found between the no-injection and day 7 hUTC treatment groups ($p = 0.0178$). There was no significant difference between the no-injection and day 7 vehicle treatment groups. Representative images of IB4-stained choroidal flat-mounts from these three treatment groups (no injection, day 7 vehicle, and day 7 hUTC) are shown in Figure 1C, and they reflect the differences in LCNV lesion size among these groups. Subretinal injections at 0, 14, or 28 days pre-laser treatment yielded no significant differences between vehicle and hUTC groups (Figure 1). Lesions sizes were measured from between 9 and 11 retinas for each treatment group.

Inhibition of LCNV-Induced VEGF by hUTCs *In Vivo*

Subretinal injections of hUTCs and vehicle were performed 7 days pre-laser; VEGF levels in choroidal tissues were assessed 3 days post-laser treatment. Laser treatment significantly elevated VEGF protein levels in choroidal tissues; the mean ± SEM (picogram VEGF per milligram total tissue protein) of the non-injected LCNV group was 69.23 ± 12.41 pg/mg compared to 29.80 ± 6.57 pg/mL for the non-injected and non-laser-treated group ($p = 0.0246$). The levels in LCNV rats receiving vehicle and hUTCs were 52.56 ± 7.64 pg/mg and 10.62 ± 3.21 pg/mg ($p = 0.0252$), respectively. We observed a consistent, but statistically insignificant, downward trend in VEGF levels for LCNV rats receiving vehicle injection versus non-injection. Notably, VEGF levels in LCNV rats receiving hUTCs were lower compared to the non-injected, non-laser-treated control group (e.g., below baseline). These results are summarized in Figure 2. Biologically independent samples taken from three or four retinas in each treatment group were assayed, with three technical replicates for each sample.

Inhibition of VEGF Release from ARPE-19 by hUTCs

RPE cells are a proven source of retinal VEGF production *in vivo*, suggesting that RPE cells may contribute to neovascularization in

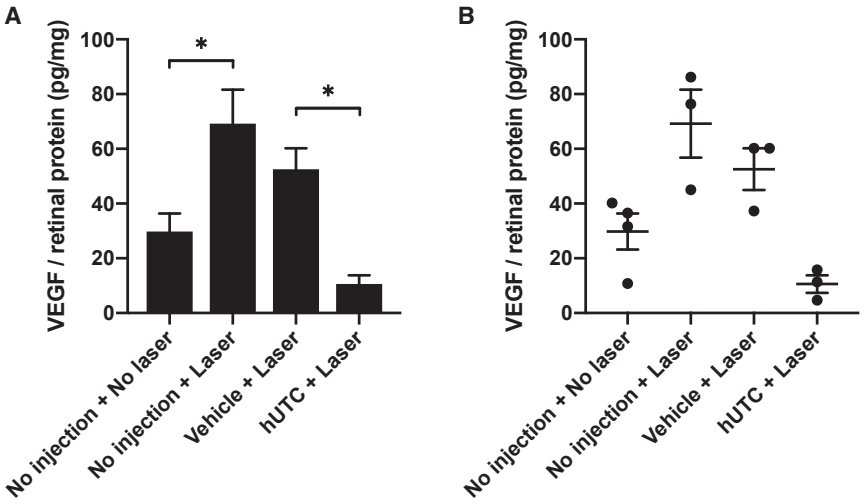

Figure 2. hUTCs Reduced Choroidal VEGF Level *In Vivo*

(A and B) Rats were treated with a subretinal injection of vehicle or hUTCs 7 days prior to laser application, or they were assigned to no-laser and/or no-injection control groups. Rats were sacrificed 3 days post-laser, and VEGF protein levels in choroidal tissue were measured by ELISA. Biologically independent samples taken from three or four retinas in each treatment group were assayed, with three technical replicates for each sample. VEGF protein levels were significantly elevated by laser application for no-injection groups ($p = 0.0246$). VEGF protein levels were significantly lowered by hUTC injection, when compared to the vehicle control group ($p = 0.0252$). Data represent mean ± SEM in bar graph (A) and scatter plot (B) format. *$p < 0.1$.

angiogenic ocular disorders.[5–7] To examine the effect of hUTCs on RPE VEGF production *in vitro*, ARPE-19 cells were cultured with or without dose-dependently seeded hUTCs. VEGF was secreted at around 220 pg/mL from ARPE-19 cultured alone 2 days post-seeding, decreased dramatically from ARPE-19 co-cultured with hUTCs, and became completely undetectable when a high density (30×10^3 or 60×10^3 cells/well) of hUTCs were seeded (Figure 3A). Moreover, when ARPE-19 CM was incubated with hUTC CM, the detectable VEGF in ARPE-19 CM was reduced markedly and rapidly in 5 min, and VEGF became completely undetectable in 2 days (Figure 3B). The level of VEGF in hUTC CM was under the detection limit (data not shown). Similarly, recombinant human VEGF (rhVEGF), when added in hUTC CM at 300 pg/mL, became negligible after 5-min incubation and undetectable in 2 days (Figure 3C). These findings suggest that some factor(s) in the hUTC CM may be able to immediately degrade or bind to VEGF and, therefore, cause VEGF to be degraded or become undetectable.

Proteases can have several distinct effects on VEGF, including cleavage, activation, liberation from extracellular stores, and degradation.[29] VEGF cleavage can occur readily via the proteases plasmin and matrix metalloproteinases (MMPs).[30,31] To examine the possibility of proteolytic degradation of VEGF, hUTC CM was pretreated with a broad spectrum of protease inhibitor cocktail for 30 min before rhVEGF (300 pg/mL) was added and incubated for 5 min. However, the pre-incubation of hUTC CM with protease inhibitor cocktail had no effect on the decrease of rhVEGF (Figure 3D). Similarly, rhVEGF was below detectable levels in hUTC CM with or without protease inhibitor cocktail after further incubation for 15, 30, 60, or 120 min (data not shown). This suggests that proteases are not involved in the VEGF reduction in hUTC CM.

Identification of VEGF-Binding Factor(s) in hUTC CM

Many factors have been reported to bind to VEGF, such as neuropilin-2, thrombospondin, connective tissue growth factor, platelet factor-4, alpha 2-macroglobulin, collagen, and heparin sulfate proteoglycan.[32–38] In an effort to identify the factors bound to VEGF in culture medium, we prepared immunoprecipitation fractions from hUTC CM and control medium using a VEGF pull-down assay. Proteins in hUTC CM that bound to VEGF were pulled down by rhVEGF-conjugated beads. The protein-bead complex was then eluted in buffers. Part of the eluate was used for western blot analysis, and the remaining eluate was further processed for MS analysis. Protein identification was accomplished by liquid chromatography-tandem MS (LC-MS/MS) analysis of tryptic digests of binding fractions, followed by peptide mapping and data analysis.

The only high-confidence identified protein in hUTC CM was vascular endothelial growth factor receptor 1 [*Homo sapiens*] (GenBank: gi229892300) (Table 1). The nine peptides identified provide evidence for the presence of the soluble VEGFR1 protein in the hUTC CM, but not in the control medium. The only other protein identified was porcine trypsin (GenBank: gi999627), predicated on the identification of three autolysis fragment peptides found in both the conditioned and control media (Table 1). These results suggest that hUTCs secrete the soluble form of VEGFR1 and that this protein binds VEGF. We further confirmed this by the detection of a high level of sVEGFR1 (1,739.0 ± 48.505 pg/mL) in hUTC CM using ELISA. Furthermore, the level of rhVEGF in human CM was significantly recovered when the CM was pre-incubated with a neutralizing antibody against sVEGFR1 (Figure 4).

In addition, the hUTC CM eluate from VEGF pull-down immunoprecipitation was subject to western blot analysis, and the molecular weight of sVEGFR1 in hUTC CM was evaluated. Recombinant human sVEGFR1, with a mass of approximately 96 kDa, was used as a positive control. The antibody to sVEGFR1 yielded a predominant band of ~110 kDa and a minor band of ~150 kDa in an hUTC CM sample. A single band of ~96 kDa was detected for recombinant human sVEGFR1 (Figure 5).

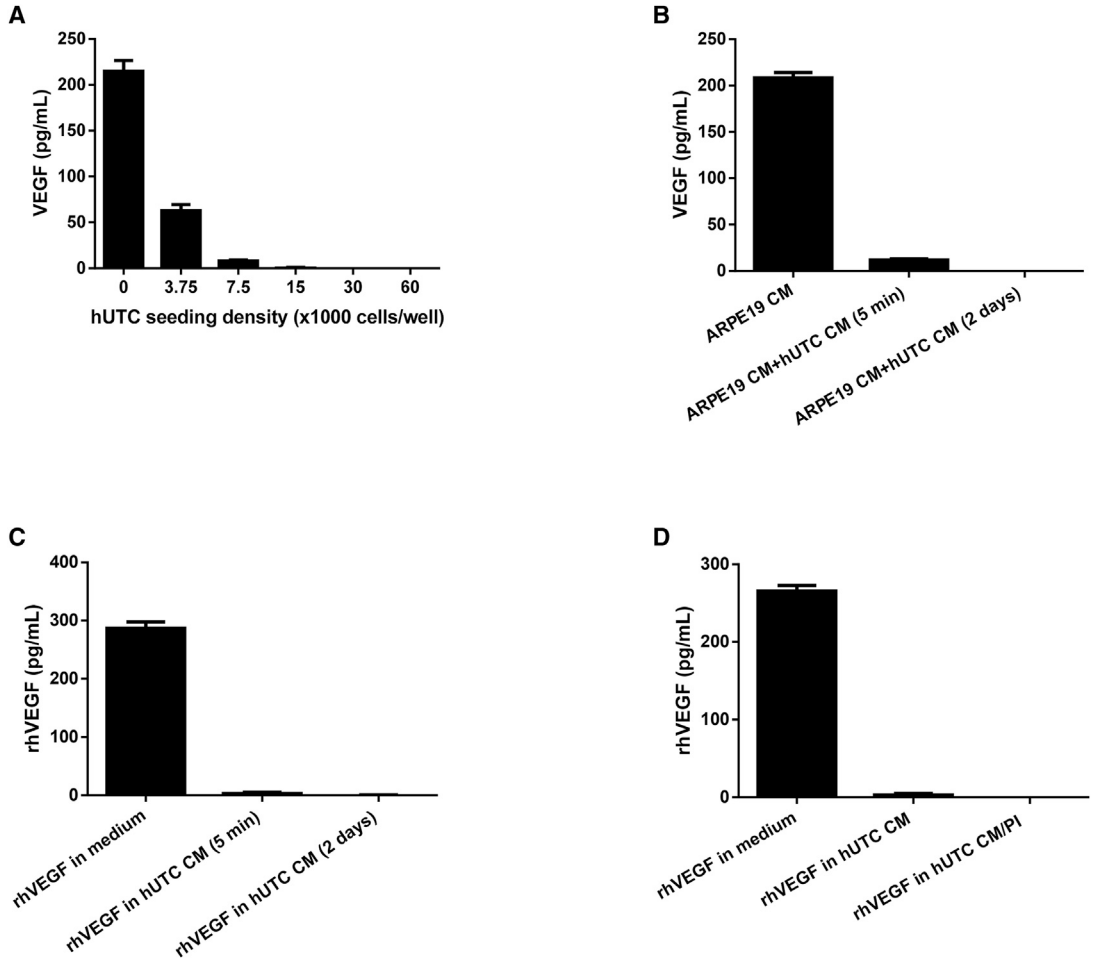

Figure 3. hUTCs Reduced VEGF *In Vitro*

(A) ARPE-19 cells were seeded at 60 × 10^3 cells/well in a 24-well plate and cultured with or without density-dependent hUTCs for 48 h, followed by VEGF measurement by ELISA. (B) Conditioned media were collected from ARPE-19 cells and hUTCs cultured individually in a 24-well plate, then mixed at a 1:1 ratio, and cultured for 5 min and 2 days, respectively, at 37°C, followed by VEGF measurement. (C) Recombinant human VEGF (300 pg/mL) was added to hUTC CM and incubated for 5 min and 2 days, respectively, at 37°C, followed by VEGF measurement. (D) rhVEGF (300 pg/mL) was added to hUTC CM preincubated with a broad-spectrum protease inhibitor cocktail and cultured at 37°C for 5 min. VEGF was then measured by ELISA. Data represent mean ± SEM (n = 3).

Taken together, the above findings strongly indicate that sVEGFR1 is the only factor in hUTC CM that binds to VEGF.

DISCUSSION

Prior to the advent of anti-VEGF therapy, photocoagulation and photodynamic therapies were the standard of care for neovascular AMD. These approaches are destructive, and in most cases the best outcome is stabilization of vision.[39] With the FDA approvals and clinical applications of the anti-VEGF therapies Macugen (Eyetech Pharmaceuticals/OSI Pharmaceuticals, Long Island, NY, USA) in 2004,[40] followed by bevacizumab (Avastin, Genentech, South San Francisco, CA, USA),[41] ranibizumab (Lucentis, Genentech),[42–44] and aflibercept (Eylea, Regeneron, Tarrytown, NY, USA),[39,45–47] a significant percentage of patients with neovascular AMD began to realize improvement in vision.[39] Typically, patients with wet AMD are treated with anti-VEGF therapies until subretinal fluid is not observed by optical coherence tomography (OCT) or, alternatively stated, until the patient appears dry. A significant percentage of wet AMD patients still demonstrate subretinal fluid after 3 months of multiple intravitreal injections, indicating the need for continued injections.[48] Even after subretinal fluid no longer persists, varied continued treatment strategies may be implemented, including the wait-and-see or treat-and-extend protocols.[48,49] These are intended to eliminate any residual or prevent the reoccurrence of subretinal fluid. Regardless of the approach, patients affected with wet AMD find themselves having to endure an indefinite number of repeated intravitreal injections of anti-VEGF drugs, along with their associated risk factors, including the development of endopthalmitis and reduced patient compliance.[50–54]

Table 1. Proteins Identified in the hUTC Conditioned Medium and Control Medium

Sample	GenBank Accession Number	Identified Protein	Number of Peptides[a]
Control medium	gi999627	trypsin, porcine	3
hUTC conditioned medium	gi229892300	vascular endothelial growth factor receptor 1 (*Homo sapiens*)	9
	gi999627	trypsin, porcine	3

[a]Two or more peptides are required for high-confidence protein identification.

We propose that anti-angiogenic cell-based therapies may offer a solution to these drawbacks. For example, cells secreting high levels of anti-angiogenic factors could be transplanted to the subretinal space, where they are stably integrated, releasing these factors on a prolonged basis. If such a therapy could be achieved, the problems associated with relapsing pathology due to cessation of therapy and/or multiple intravitreal injections associated with prophylaxis could be avoided. We chose to use subretinal injection in this study, primarily to increase the likelihood that hUTC-secreted factors would be bioavailable at the site of CNV occurrence. Notably, although rare, there are adverse events associated with subretinal injection, including retinal detachment, vitreous hemorrhage, recurrence of submacular hemorrhage, and postoperative development of CNV.[55,56]

This study yielded data suggesting the feasibility of a cell-based anti-angiogenic therapy against wet AMD. Rodent models of LCNV have been used to test a broad range of potential CNV therapies, including those targeting VEGF.[57–60] We tested hUTCs via subretinal injection in the rat model, and we observed an approximate 33% reduction of LCNV compared to vehicle controls. Increased VEGF levels are routinely observed in choroidal tissues of LCNV rats, presumably eliciting the neovascular response;[61] therefore, we assayed VEGF levels to determine any possible effect of hUTCs. Indeed, choroidal VEGF was reduced in LCNV rats receiving hUTCs via subretinal injection. The pre-laser injection times of hUTCs used in our *in vivo* VEGF assays were the same as those used in our LCNV efficacy experiments. However, VEGF was assayed at 3 days and LCNV lesion area at 14 days post-laser treatment. An increase in VEGF prior to the onset of the vasoproliferative response is a common finding in experimental models of ocular vasculopathies.[14,16,58,61–64] These findings are consistent with the hypothesis that hUTC angiostatic bioactivity is due to their VEGF-lowering capacity.

We performed *in vitro* experiments to elucidate any molecular mechanisms that could explain hUTC-dependent decreases in the pathology and VEGF levels we observed in LCNV rats. Several lines of evidence suggest that RPE-derived VEGF is likely to drive the development of neovascular AMD.[42,60,65–69] Therefore, we performed co-culture and CM experiments to test whether hUTCs had any effects on the VEGF levels produced by ARPE-19 cells, and we found

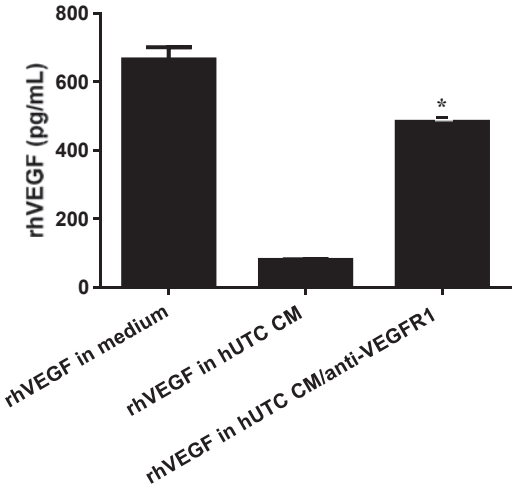

Figure 4. Neutralizing Antibody against sVEGFR1 Recovers the VEGF Level in hUTC Conditioned Medium

hUTC conditioned medium was pre-incubated with a neutralizing antibody (10 ug/mL) against sVEGFR1 for 1 h at 37°C, followed by the addition of rhVEGF at 1 ng/mL, and incubated for another 30 min. VEGF level was measured by ELISA. Data represent mean ± SEM (n = 3). *$p < 0.05$.

that they were reduced by hUTC CM. We used VEGF pull-down assays coupled with MS analysis to identify sVEGFR1 as a potential causative factor. We detected two sVEGFR1 immunoreactive bands shown in a representative western blot (Figure 5). The major band at 110 kDa is also detected in human umbilical vein endothelial cells and primary human dermal microvascular endothelial cells.[70] The minor band at approximately 150 kDa may be a variant resulting from differences in glycosylation.[71] Molecular weight differences in sVEGFR1 have been reported and attributed to differences in this post-translation modification.[70,71]

LCNV and choroidal VEGF tissue levels were reduced in rats receiving hUTCs via subretinal injection, and our *in vitro* data suggest that sVEGF1 released from these transplanted cells is responsible. Aflibercept is a VEGF trap that has a higher affinity for all the VEGF isoforms when compared to bevacizumab and ranibizumab.[45–47] Evidence suggests that it may be superior in cases in which recalcitrant CNV is observed.[72] It is akin to hUTC-derived sVEGFR1 in that it is a chimera constructed of sequences from human VEGFR1 and VEGFR2. Notably, the results we obtained from testing hUTCs against rat LCNV compare favorably to those of pre-clinical studies testing intraocular injection of aflibercept in the same model, in which an approximate 22% reduction in LCNV was observed.[67] In a head-to-head comparison, Macugen, bevacizumab, and ranibizumab (all targeting human VEGF) were tested in rat LCNV by intravitreal injection, and each showed no efficacy against fluid leakage associated with LCNV.[72] In light of these findings, we speculate that increased efficacy may have been observed in the current study had we tested the rat equivalent of hUTCs, releasing the rat sVEGR1 homolog.

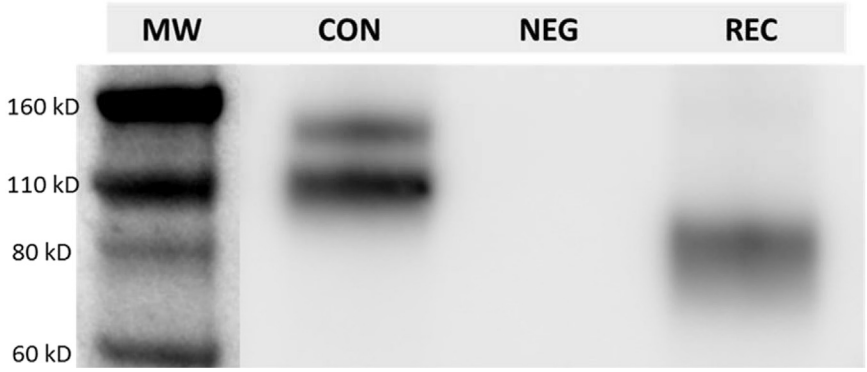

Figure 5. Western Blot Analysis of sVEGFR1 in hUTC Conditioned Medium

The eluates of hUTC CM and control medium from VEGF pull-down assay were subject to SDS-PAGF. Briefly, 40 uL Tris-eluate solution mixed with sample buffer and 25 ng recombinant human soluble VEGFR1 were run on an SDS-PAGE gel, and the gel-resolved proteins were transferred onto a PVDF membrane. The membrane was blocked with 5% (w/v) BSA, and subsequently it was probed with a biotinylated anti-VEGFR1 antibody targeting the extracellular region of VEGFR1. After washing, the membrane was incubated with streptavidin-HRP, and immunoreactive bands were visualized with enhanced chemiluminescence (ECL). CON, hUTC control medium sample; NEG, negative control (control medium); REC, recombinant human sVEGFR1.

Retinal degeneration, a feature of dry AMD, is observed in Royal College of Surgeons (RCS) rat. In a previous study, we found that hUTCs rescue the phagocytic defect of RPE cells isolated from these rats by expressing and secreting trophic factors, including brain-derived neurotrophic factor, hepatocyte growth factor, and glial cell-derived neurotrophic factor.[73] Upon consideration of these data, we were not compelled to test for hUTC-related retinal toxicity in the current study. Furthermore, we did not observe any evidence of increased inflammation in rat eyes receiving hUTCs by subretinal injection, beyond that associated with laser-induced rupture of Bruch's membrane and the vehicle injection.

These combined data from previous and the current studies suggest that an hUTC-based therapy could provide intervention at both the dry and wet stages of AMD while eliminating some common drawbacks associated with the current anti-VEGF therapies. Future studies will be directed at tracking hUTC behavior at the molecular and cellular levels over time to enhance their therapeutic benefit over periods of progressively longer duration in animal models of retinal and choroidal disease.

MATERIALS AND METHODS

Materials

The VEGF ELISA kit was from Thermo Scientific (Pittsburgh, PA). sVEGFR1 and rat VEGF ELISA kits were from R&D Systems (Minneapolis, MN). Recombinant human VEGF165 (a 165-amino acid splice variant of VEGF) was from EMD Chemicals (Gibbstown, NJ). Halt Protease inhibitor Single-Use Cocktail was obtained from Thermo Scientific (Pittsburgh, PA) and used at 1× or 3× the concentrations, as instructed by the vendor. Anti-human VEGFR1 antibodies (AF321 and BAF321) and normal goat immunoglobulin G (IgG) isotype control antibody were from R&D Systems (Minneapolis, MN). Recombinant human sVEGFR1 was from Cell Science (Canton, MA). Alexa Flour-conjugated Griffonia simplicifolia IB4 was obtained from Thermo Fisher Scientific (Waltham, MA), and anti-elastin was from Abcam (Cambridge, MA). Rat VEGF ELISA was obtained from R&D Systems (Minneapolis, MN).

Animals and Treatments

All procedures were performed with strict adherence to guidelines for animal use and experimentation set forth by the Vanderbilt University Animal Care and Use Committee and the Association for Research in Vision and Ophthalmology.

Subretinal Injections

The 6-week-old male Brown Norway rats (Charles River Laboratories, Wilmington, MA) were anesthetized with an intraperitoneal (i.p.) injection of ketamine (80 mg/kg)/xylazine (8 mg/kg) (Henry Schein, Melville, NY). Their pupils were dilated with 1% tropicamide (Alcon Pharmaceuticals, Ft. Worth, TX); they were placed in lateral recumbency under a Zeiss Operating Microscope (Zeiss, Peabody, MA), and the head was immobilized by holding it with one hand. GenTeal lubricant eye gel (Alcon Pharmaceuticals) was applied to the corneal surface and the fundus was visualized. A guide hole for the delivery of hUTCs was prepared as follows: while proptosing the eye, the globe was punctured with a 19°-beveled 30G needle (Hamilton, Reno, NV) immediately posterior to the corneal limbus at a steep angle to avoid touching the lens. The needle was retracted while keeping the head immobilized. A Hamilton syringe fitted with a 33G blunt-ended needle (Hamilton) was pre-loaded with 2 μL hUTC suspension. This needle was inserted into the guide hole at a steep angle to avoid contact with the lens and advanced through the eye until penetration of the retina and entrance into the subretinal space. The syringe was held in place by one operator while another slowly delivered its contents into the subretinal space, creating a visible retinal detachment. Following subretinal delivery, the needle was gently withdrawn. Immediately following the injection procedure, 2–3 drops of a 0.3% Tobramycin Ophthalmic Solution USP (Allivet, Miami, FL) was applied to the anterior surface of eye to prevent infection.

Four subretinal injection protocols were tested as follows: rats received subretinal injections of hUTCs or vehicle at 28, 14, or 7 days prior to laser treatment or at the time of laser treatment (0 days). CNV measurements were conducted 14 days post-laser treatment. For choroidal VEGF measurements, rats were treated with a subretinal injection of vehicle or hUTCs 7 days prior to laser

application, or they were assigned to no-laser and/or no-injection control groups. Rats were sacrificed 3 days post-laser treatment, and VEGF protein levels in choroidal tissue were measured by ELISA.

LCNV

Rats were anesthetized with an i.p. injection of ketamine (80 mg/kg)/(8 mg/kg) xylazine (Henry Schein). The pupils were dilated with 1% tropicamide (Alcon Pharmaceuticals). Using a hand-held coverslip as a contact lens and GenTeal lubricating eye gel (Alcon Pharmaceuticals) as a medium contacting the coverslip and the service of the cornea, an AC-2000 argon laser photocoagulator operating at 488/514 nm (NIDEK, Fremont CA) coupled to a SL-1600 slit-lamp (NIDEK) was used to create four Bruch's membrane-penetrating burns equidistant from the optic nerve head in the retinal mid-periphery. Lesions were created with laser parameters that included 100-μm spot size, 0.1-s duration, and 120 mW.

Choroidal Flat-Mounts and Tissue Staining

Choroidal mounts and tissue staining were performed in a manner similar to that described by Bora et al.[74] Rats were deeply anesthetized and euthanized by cervical dislocation. The eyes were then enucleated and placed in 10% formalin (Sigma) for 2 h. The RPE-choroid-sclera complexes were obtained by hemisecting the eyes, removing the lens, and peeling the neural retina away from the underlying RPE. At least four radial cuts were made to allow this tissue to be flattened. Constituent endothelial cells of choroidal neovascular lesions were identified with IB4 (Sigma), while the elastin of the extracellular matrix was identified using goat anti-elastin antibody conjugated to Cy3 (Santa Cruz Biotechnology, Santa Cruz, CA). The flat-mount was then placed onto a microscope slide with the RPE side facing up. Gel Mount medium (Biomeda) was applied to the tissue before covering the slide with a coverslip. Choroidal mounts were visualized using the 10× objective of an epifluorescent compound microscope fitted with the appropriate excitation and emission filters (Provis AX-70, Olympus, Japan). Images of the neovascular lesions were captured using a digital camera attached to the Provis system (DP71, Olympus, Japan) with image capture software (DP Controller, Olympus, Japan).

Neovascular Lesion Area Measurement

Images of the neovascular lesions were opened in Adobe Photoshop. Lesion areas were selected by observers masked to treatment using a combination of the magic wand tool, with tolerance set at 40, and the lasso tool. The total area, in pixels, of the selection was obtained within the histogram view, and it was later converted to squared millimeters using the scale bar feature of the image-capturing software.

Choroidal VEGF Level Measurement

Laser-induced rupture of Bruch's membrane was used to generate CNV in 6-week-old male Brown Norway rats. Rats were divided into treatment arms that included non-laser control, laser plus no injection, vehicle injection, and hUTC injection administered 7 days pre-laser. Choroidal tissues were dissected at 3 days post-laser treatment and homogenized, and VEGF protein was measured using a rat VEGF ELISA (R&D Systems, RRV00). VEGF protein levels were normalized to total protein in the choroidal tissues. Collected tissues included choroid, Bruch's membrane, and RPE.

hUTC Culture

hUTCs were isolated, cultured, and cryopreserved as previously described.[35] Briefly, human umbilical cords were obtained with donor consent following live births from the National Disease Research Interchange (Philadelphia, PA). Tissues were minced and enzymatically digested at 37°C, shaking for around 3 h until most (~90%) of the tissue had been digested. After almost complete digestion with a DMEM-low glucose (LG) medium (Invitrogen, Carlsbad, CA), containing a mixture of 0.5 U/mL collagenase (Serva Electrophoresis), 5 U/mL neutral protease (Serva Electrophoresis), and 2 U/mL hyaluronidase (Cumulase, Origio), the cell suspension was filtered through a 70-μm filter, and the supernatant was centrifuged at 350 × *g*. Isolated cells were washed in DMEM-LG a few times and seeded at a density of 5,000 cells/cm^2 in DMEM-LG medium, containing 15% (v/v) fetal bovine serum (FBS) (HyClone, Logan, UT) and 4 mM L-glutamine (Gibco, Grand Island, NY). When cells reached approximately 70% confluence, they were passaged using TrypLE (Gibco, Grand Island, NY). Cells were harvested after two to three passages and banked.

Preparation of hUTC and ARPE-19 CM

On day 1, hUTCs or ARPE-19 cells were thawed and plated in a 6-well plate at 0.288 × 10^6 cells/2.4 mL/well in DMEM-LG medium containing 15% (v/v) FBS (HyClone, Logan, UT) and 4 mM L-glutamine (Gibco, Grand Island, NY). On day 2, medium was aspirated and replenished with DMEM/F12 medium (ATCC) containing 10% v/v FBS, 50 U/mL penicillin (Invitrogen), and 50 μg/mL streptomycin (Invitrogen). Cells remained in these culture conditions for 48 h, after which CM from hUTCs or ARPE-19 cells was collected to be used for experiments or frozen at −70°C for future use.

Co-culture of hUTCs with ARPE-19 Cells

hUTCs were plated at various densities (0, 3.75, 7.5, 15, 30, and 60 × 10^3 cells/1 mL/well) in a 24-well plate in DMEM (LG; Invitrogen, Carlsbad, CA), containing 15% v/v FBS (HyClone, Logan, UT), 50 U/mL penicillin, 50 μg/mL streptomycin (Invitrogen, Carlsbad, CA), and 4 mM glutamine (Invitrogen, Carlsbad, CA). After 24 h in culture, ARPE-19 cells were then plated on top of hUTCs (60 × 10^3 cells/1 mL/well in a 24-well plate) in DMEM/F12 medium (Invitrogen, Carlsbad, CA), containing 10% v/v FBS, 50 U/mL penicillin, and 50 μg/mL Streptomycin. After 24 h of co-culture, media were aspirated and replenished with fresh media (0.5 mL/well). Cell culture supernatants were collected in 24 h followed by VEGF measurement by ELISA.

Immunoprecipitation

10 μg recombinant human VEGF165 (PeproTech, Princeton, NJ)/mg Dynabeads (Thermo Fisher Scientific, Rochester, NY) was conjugated, per the manufacturer's directions, for a final concentration of 10 mg beads/mL (100 μg VEGF/mL). 15 mL hUTC CM or control medium was mixed with 0.3 mg VEGF-conjugated bead solution. Samples were

incubated by rolling for 30 min at 4°C and washed with a buffer (100 mM Tris, [pH 7.4], 100 mM NaCl, 100 mM KCl, 1 mM $MgCl_2$, 1 mM $CaCl_2$, 1 mM EDTA buffer, and 1% protease inhibitors). Samples were then eluted in 50 μL 50 mM HCL for 5 min, and the eluates were finally mixed with 5 μL 1.0 M Tris (pH 8.5). For western blot analysis, 40 μL Tris-eluate solution mixed with NuPAGE LDS Sample Buffer (4×) (Life Technologies, Carlsbad, CA) and 25 ng recombinant human soluble VEGFR1 were submitted to SDS-PAGE, and the gel-resolved proteins were transferred onto a polyvinylidene difluoride (PVDF) membrane. The membrane was blocked with 5% (w/v) BSA, and subsequently it was probed with a biotinylated anti-VEGFR1 antibody (R&D Systems, Minneapolis, MN), targeting the extracellular region of VEGFR1. After washing, the membrane was incubated with streptavidin-horseradish peroxidase (HRP) (Jackson ImmunoResearch Laboratories, West Grove, PA), and immunoreactive bands were visualized with enhanced chemiluminescence western blotting substrate. The remaining eluate was used for MS analysis to identify VEGF-binding factors in hUTC CM.

MS

Two immunoprecipitation pull-down samples, prepared from hUTC CM and control medium (medium alone), were processed for MS analysis. The samples were concentrated, reduced, alkylated, and digested. Protein identification was then done using tryptic digestions of binding fractions, followed by peptide mapping and data analysis.

R&A Peptide Digestion

The samples (~150 μL each) were concentrated to approximately 15 μL in a vacuum centrifuge. They were reduced (R) by mixing with 2 μL 100 mM dithiothreitol (DTT), after which the solution was incubated at 60°C for 30 min. After reduction, the samples were alkylated (A) by adding 2 μL 100 mM iodoacetamide (IAA) and incubating at room temperature (RT) in the dark for 20 min. Finally, a 1.0 μL aliquot of trypsin ([C] = 0.5 μg/μL) was added, and the solutions were digested overnight (~16 h) at 37°C.

High-Performance Liquid Chromatography (HPLC)-MS Data Generation

The peptide digests were analyzed using a Dionex U3000 HPLC coupled with a Bruker Daltonics micrOTOF-Q II mass spectrometer. An 18 μL aliquot of sample was injected for each analysis. The digests were separated using an LC Packings Acclaim PepMap C_{18}, 180 μm × 150 mm, 3 μm d_p column; solvent A was 0.1% formic acid (FA) in water and solvent B was acetonitrile. The column was maintained at a temperature of 65°C. The flow rate was 6.0 μL/min, and the flow passed directly into the micrOTOF mass spectrometer. The electrospray emitter was held at ground, the transfer capillary voltage was −4.5 kV, and the end plate offset voltage was set at −500 V. One analysis was performed per sample: the top 5 data-directed analysis (DDA) with precursors selected from the mass range *m/z* 400–1,700.

Data Analysis

The results were searched against the NCBI non-redundant database (October 2, 2011 release) with human taxonomy. Identified proteins listed in Table 1 were made from peptide MS/MS data with a significance of $p < 0.05$ and the expectation threshold was set at ≤ 0.05.

Statistical Analysis

For *in vivo* efficacy and VEGF protein studies, statistical significance was assessed by ANOVA coupled with a Student's t test post hoc analysis. A p value <0.05 was considered statistically significant. All illustrations and statements of variability refer to SEM.

AUTHOR CONTRIBUTIONS

J.C. conceived and designed the study, designed and performed the experiments, provided study materials, collected and assembled data, performed data analysis and interpretation, and wrote and edited the manuscript. R.Y. performed subretinal injection, choroid dissection, and retinal VEGF ELISA. T.E.S. collected and assembled *in vivo* data, conducted data analysis, and edited the manuscript. S.E. performed animal injection and tissue staining. G.W.M. designed the study, interpreted data, and wrote the manuscript. S.C.P. performed mass spectrometry and data analysis. T.P. performed immunoprecipitation. I.R.H. conceived the study. J.S.P. designed the study, collected and assembled *in vivo* data, conducted data analysis and interpretation, and wrote and edited the manuscript.

CONFLICTS OF INTEREST

The authors declare no competing interests.

ACKNOWLEDGMENTS

We thank Michael Naso and Jennifer Nemeth-Seay (Janssen R&D, Spring House, PA) for providing advisory suggestions and Eilyn Lacy (Janssen R&D, Spring House, PA) for assistance with VEGF-binding factor identification. This work was performed under a sponsored research agreement between Vanderbilt University School of Medicine and Janssen R&D.

REFERENCES

1. de Jong, P.T. (2006). Age-related macular degeneration. N. Engl. J. Med. *355*, 1474–1485.
2. Ambati, J., Ambati, B.K., Yoo, S.H., Ianchulev, S., and Adamis, A.P. (2003). Age-related macular degeneration: etiology, pathogenesis, and therapeutic strategies. Surv. Ophthalmol. *48*, 257–293.
3. Dadgostar, H., and Waheed, N. (2008). The evolving role of vascular endothelial growth factor inhibitors in the treatment of neovascular age-related macular degeneration. Eye (Lond.) *22*, 761–767.
4. Bressler, S.B. (2009). Introduction: Understanding the role of angiogenesis and anti-angiogenic agents in age-related macular degeneration. Ophthalmology *116* (10, Suppl), S1–S7.
5. Lu, M., and Adamis, A.P. (2006). Molecular biology of choroidal neovascularization. Ophthalmol. Clin. North Am. *19*, 323–334.
6. Stewart, M.W. (2012). Clinical and differential utility of VEGF inhibitors in wet age-related macular degeneration: focus on aflibercept. Clin. Ophthalmol. *6*, 1175–1186.
7. McLeod, D.S., Grebe, R., Bhutto, I., Merges, C., Baba, T., and Lutty, G.A. (2009). Relationship between RPE and choriocapillaris in age-related macular degeneration. Invest. Ophthalmol. Vis. Sci. *50*, 4982–4991.
8. Grossniklaus, H.E., Martinez, J.A., Brown, V.B., Lambert, H.M., Sternberg, P., Jr., Capone, A., Jr., Aaberg, T.M., and Lopez, P.F. (1992). Immunohistochemical and

histochemical properties of surgically excised subretinal neovascular membranes in age-related macular degeneration. Am. J. Ophthalmol. *114*, 464–472.

9. Frank, R.N., Amin, R.H., Eliott, D., Puklin, J.E., and Abrams, G.W. (1996). Basic fibroblast growth factor and vascular endothelial growth factor are present in epiretinal and choroidal neovascular membranes. Am. J. Ophthalmol. *122*, 393–403.

10. Kvanta, A., Algvere, P.V., Berglin, L., and Seregard, S. (1996). Subfoveal fibrovascular membranes in age-related macular degeneration express vascular endothelial growth factor. Invest. Ophthalmol. Vis. Sci. *37*, 1929–1934.

11. Lopez, P.F., Sippy, B.D., Lambert, H.M., Thach, A.B., and Hinton, D.R. (1996). Transdifferentiated retinal pigment epithelial cells are immunoreactive for vascular endothelial growth factor in surgically excised age-related macular degeneration-related choroidal neovascular membranes. Invest. Ophthalmol. Vis. Sci. *37*, 855–868.

12. Kuroki, M., Voest, E.E., Amano, S., Beerepoot, L.V., Takashima, S., Tolentino, M., Kim, R.Y., Rohan, R.M., Colby, K.A., Yeo, K.T., and Adamis, A.P. (1996). Reactive oxygen intermediates increase vascular endothelial growth factor expression in vitro and in vivo. J. Clin. Invest. *98*, 1667–1675.

13. Lu, M., Kuroki, M., Amano, S., Tolentino, M., Keough, K., Kim, I., Bucala, R., and Adamis, A.P. (1998). Advanced glycation end products increase retinal vascular endothelial growth factor expression. J. Clin. Invest. *101*, 1219–1224.

14. Baffi, J., Byrnes, G., Chan, C.C., and Csaky, K.G. (2000). Choroidal neovascularization in the rat induced by adenovirus mediated expression of vascular endothelial growth factor. Invest. Ophthalmol. Vis. Sci. *41*, 3582–3589.

15. Schwesinger, C., Yee, C., Rohan, R.M., Joussen, A.M., Fernandez, A., Meyer, T.N., Poulaki, V., Ma, J.J., Redmond, T.M., Liu, S., et al. (2001). Intrachoroidal neovascularization in transgenic mice overexpressing vascular endothelial growth factor in the retinal pigment epithelium. Am. J. Pathol. *158*, 1161–1172.

16. Spilsbury, K., Garrett, K.L., Shen, W.Y., Constable, I.J., and Rakoczy, P.E. (2000). Overexpression of vascular endothelial growth factor (VEGF) in the retinal pigment epithelium leads to the development of choroidal neovascularization. Am. J. Pathol. *157*, 135–144.

17. Hicklin, D.J., and Ellis, L.M. (2005). Role of the vascular endothelial growth factor pathway in tumor growth and angiogenesis. J. Clin. Oncol. *23*, 1011–1027.

18. Wu, F.T., Stefanini, M.O., Mac Gabhann, F., Kontos, C.D., Annex, B.H., and Popel, A.S. (2010). A systems biology perspective on sVEGFR1: its biological function, pathogenic role and therapeutic use. J. Cell. Mol. Med. *14*, 528–552.

19. Holz, F.G., Schmitz-Valckenberg, S., and Fleckenstein, M. (2014). Recent developments in the treatment of age-related macular degeneration. J. Clin. Invest. *124*, 1430–1438.

20. Hanout, M., Ferraz, D., Ansari, M., Maqsood, N., Kherani, S., Sepah, Y.J., Rajagopalan, N., Ibrahim, M., Do, D.V., and Nguyen, Q.D. (2013). Therapies for neovascular age-related macular degeneration: current approaches and pharmacologic agents in development. BioMed Res. Int. *2013*, 830837.

21. Costagliola, C., Agnifili, L., Arcidiacono, B., Duse, S., Fasanella, V., Mastropasqua, R., Verolino, M., and Semeraro, F. (2012). Systemic thromboembolic adverse events in patients treated with intravitreal anti-VEGF drugs for neovascular age-related macular degeneration. Expert Opin. Biol. Ther. *12*, 1299–1313.

22. Bhattacharya, S., Gangaraju, R., and Chaum, E. (2017). Recent Advances in Retinal Stem Cell Therapy. Curr. Mol. Biol. Rep. *3*, 172–182.

23. Tang, Z., Zhang, Y., Wang, Y., Zhang, D., Shen, B., Luo, M., and Gu, P. (2017). Progress of stem/progenitor cell-based therapy for retinal degeneration. J. Transl. Med. *15*, 99.

24. Ho, A.C., Chang, T.S., Samuel, M., Williamson, P., Willenbucher, R.F., and Malone, T. (2017). Experience with a subretinal cell-based therapy in patients with geographic atrophy secondary to age-related macular degeneration. Am. J. Ophthalmol. *179*, 67–80.

25. Gehrs, K.M., Anderson, D.H., Johnson, L.V., and Hageman, G.S. (2006). Age-related macular degeneration–emerging pathogenetic and therapeutic concepts. Ann. Med. *38*, 450–471.

26. Holz, F.G., Strauss, E.C., Schmitz-Valckenberg, S., and van Lookeren Campagne, M. (2014). Geographic atrophy: clinical features and potential therapeutic approaches. Ophthalmology *121*, 1079–1091.

27. Sunness, J.S., Gonzalez-Baron, J., Applegate, C.A., Bressler, N.M., Tian, Y., Hawkins, B., Barron, Y., and Bergman, A. (1999). Enlargement of atrophy and visual acuity loss in the geographic atrophy form of age-related macular degeneration. Ophthalmology *106*, 1768–1779.

28. Ambati, J., Atkinson, J.P., and Gelfand, B.D. (2013). Immunology of age-related macular degeneration. Nat. Rev. Immunol. *13*, 438–451.

29. Vempati, P., Popel, A.S., and Mac Gabhann, F. (2014). Extracellular regulation of VEGF: isoforms, proteolysis, and vascular patterning. Cytokine Growth Factor Rev. *25*, 1–19.

30. Lee, S., Jilani, S.M., Nikolova, G.V., Carpizo, D., and Iruela-Arispe, M.L. (2005). Processing of VEGF-A by matrix metalloproteinases regulates bioavailability and vascular patterning in tumors. J. Cell Biol. *23*, 681–691.

31. Vempati, P., Mac Gabhann, F., and Popel, A.S. (2010). Quantifying the proteolytic release of extracellular matrix-sequestered VEGF with a computational model. PLoS ONE *5*, e11860.

32. Gluzman-Poltorak, Z., Cohen, T., Herzog, Y., and Neufeld, G. (2000). Neuropilin-2 is a receptor for the vascular endothelial growth factor (VEGF) forms VEGF-145 and VEGF-165 [corrected]. J. Biol. Chem. *275*, 18040–18045.

33. Gupta, K., Gupta, P., Wild, R., Ramakrishnan, S., and Hebbel, R.P. (1999). Binding and displacement of vascular endothelial growth factor (VEGF) by thrombospondin: effect on human microvascular endothelial cell proliferation and angiogenesis. Angiogenesis *3*, 147–158.

34. Inoki, I., Shiomi, T., Hashimoto, G., Enomoto, H., Nakamura, H., Makino, K., Ikeda, E., Takata, S., Kobayashi, K., and Okada, Y. (2002). Connective tissue growth factor binds vascular endothelial growth factor (VEGF) and inhibits VEGF-induced angiogenesis. FASEB J. *16*, 219–221.

35. Gengrinovitch, S., Greenberg, S.M., Cohen, T., Gitay-Goren, H., Rockwell, P., Maione, T.E., Levi, B.Z., and Neufeld, G. (1995). Platelet factor-4 inhibits the mitogenic activity of VEGF121 and VEGF165 using several concurrent mechanisms. J. Biol. Chem. *270*, 15059–15065.

36. Bhattacharjee, G., Asplin, I.R., Wu, S.M., Gawdi, G., and Pizzo, S.V. (2000). The conformation-dependent interaction of alpha 2-macroglobulin with vascular endothelial growth factor. A novel mechanism of alpha 2-macroglobulin/growth factor binding. J. Biol. Chem. *275*, 26806–26811.

37. Chen, T.T., Luque, A., Lee, S., Anderson, S.M., Segura, T., and Iruela-Arispe, M.L. (2010). Anchorage of VEGF to the extracellular matrix conveys differential signaling responses to endothelial cells. J. Cell Biol. *188*, 595–609.

38. Héroult, M., Bernard-Pierrot, I., Delbé, J., Hamma-Kourbali, Y., Katsoris, P., Barritault, D., Papadimitriou, E., Plouet, J., and Courty, J. (2004). Heparin affin regulatory peptide binds to vascular endothelial growth factor (VEGF) and inhibits VEGF-induced angiogenesis. Oncogene *23*, 1745–1753.

39. Nazari, H., Zhang, L., Zhu, D., Chader, G.J., Falabella, P., Stefanini, F., Rowland, T., Clegg, D.O., Kashani, A.H., Hinton, D.R., and Humayun, M.S. (2015). Stem cell based therapies for age-related macular degeneration: The promises and the challenges. Prog. Retin. Eye Res. *48*, 1–39.

40. Gragoudas, E.S., Adamis, A.P., Cunningham, E.T., Jr., Feinsod, M., and Guyer, D.R.; VEGF Inhibition Study in Ocular Neovascularization Clinical Trial Group (2004). Pegaptanib for neovascular age-related macular degeneration. N. Engl. J. Med. *351*, 2805–2816.

41. Bashshur, Z.F., Haddad, Z.A., Schakal, A., Jaafar, R.F., Saab, M., and Noureddin, B.N. (2008). Intravitreal bevacizumab for treatment of neovascular age-related macular degeneration: a one-year prospective study. Am. J. Ophthalmol. *145*, 249–256.

42. Rosenfeld, P.J., Brown, D.M., Heier, J.S., Boyer, D.S., Kaiser, P.K., Chung, C.Y., and Kim, R.Y.; MARINA Study Group (2006). Ranibizumab for neovascular age-related macular degeneration. N. Engl. J. Med. *355*, 1419–1431.

43. Chang, T.S., Bressler, N.M., Fine, J.T., Dolan, C.M., Ward, J., and Klesert, T.R.; MARINA Study Group (2007). Improved vision-related function after ranibizumab treatment of neovascular age-related macular degeneration: results of a randomized clinical trial. Arch. Ophthalmol. *125*, 1460–1469.

44. Brown, D.M., Michels, M., Kaiser, P.K., Heier, J.S., Sy, J.P., and Ianchulev, T.; ANCHOR Study Group (2009). Ranibizumab versus verteporfin photodynamic therapy for neovascular age-related macular degeneration: Two-year results of the ANCHOR study. Ophthalmology *116*, 57–65.e5.

45. Economides, A.N., Carpenter, L.R., Rudge, J.S., Wong, V., Koehler-Stec, E.M., Hartnett, C., Pyles, E.A., Xu, X., Daly, T.J., Young, M.R., et al. (2003). Cytokine traps: multi-component, high-affinity blockers of cytokine action. Nat. Med. *9*, 47–52.

46. Brown, D.M., Heier, J.S., Ciulla, T., Benz, M., Abraham, P., Yancopoulos, G., Stahl, N., Ingerman, A., Vitti, R., Berliner, A.J., et al.; CLEAR-IT 2 Investigators (2011). Primary endpoint results of a phase II study of vascular endothelial growth factor trap-eye in wet age-related macular degeneration. Ophthalmology *118*, 1089–1097.

47. Heier, J.S., Brown, D.M., Chong, V., Korobelnik, J.F., Kaiser, P.K., Nguyen, Q.D., Kirchhof, B., Ho, A., Ogura, Y., Yancopoulos, G.D., et al.; VIEW 1 and VIEW 2 Study Groups. (2012). Intravitreal aflibercept (VEGF trap-eye) in wet age-related macular degeneration. Ophthalmology 119, 2537–2548.

48. Jaffe, G.J., Kaiser, P.K., Thompson, D., Gibson, A., Saroj, N., Vitti, R., Berliner, A.J., and Heier, J.S. (2016). Differential Response to Anti-VEGF Regimens in Age-Related Macular Degeneration Patients with Early Persistent Retinal Fluid. Ophthalmology *123*, 1856–1864.

49. Schmidt-Erfurth, U., Kaiser, P.K., Korobelnik, J.F., Brown, D.M., Chong, V., Nguyen, Q.D., Ho, A.C., Ogura, Y., Simader, C., Jaffe, G.J., et al. (2014). Intravitreal aflibercept injection for neovascular age-related macular degeneration: ninety-six-week results of the VIEW studies. Ophthalmology *121*, 193–201.

50. Dossarps, D., Bron, A.M., Koehrer, P., Aho-Glélé, L.S., and Creuzot-Garcher, C.; FRCR net (FRenCh Retina specialists net) (2015). Endophthalmitis After Intravitreal Injections: Incidence, Presentation, Management, and Visual Outcome. Am. J. Ophthalmol. *160*, 17–25.e1.

51. Bande, M.F., Mansilla, R., Pata, M.P., Fernández, M., Blanco-Teijeiro, M.J., Piñeiro, A., and Gómez-Ulla, F. (2017). Intravitreal injections of anti-VEGF agents and antibiotic prophylaxis for endophthalmitis: A systematic review and meta-analysis. Sci. Rep. *7*, 18088.

52. Haider, M.A., Imtiaz, U., Javed, F., and Haider, Z. (2017). Incidence of acute endophthalmitis after office based intravitreal bevacizumab injection. J. Pak. Med. Assoc. *67*, 1917–1919.

53. Polat, O., İnan, S., Özcan, S., Doğan, M., Küsbeci, T., Yavaş, G.F., and İnan, Ü.Ü. (2017). Factors affecting compliance to intravitreal anti-vascular endothelial growth factor therapy in patients with age-related macular degeneration. Turk. J. Ophthalmol. *47*, 205–210.

54. Gomez, J., Koozekanani, D.D., Feng, A.Z., Holt, M., Drayna, P., Mackley, M.R., van Kuijk, F.J., Beardsley, R.M., Johnston, R.H., Terry, J.M., and Montezuma, S.R. (2016). Strategies for improving patient comfort during intravitreal injections: Results from a survey-based study. Ophthalmol. Ther. *5*, 183–190.

55. Leung, E.H., Flynn, H.W., Jr., Albini, T.A., and Medina, C.A. (2016). Retinal detachment after subretinal stem cell transplantation. Ophthalmic Surg. Lasers Imaging Retina *47*, 600–601.

56. Peng, Y., Tang, L., and Zhou, Y. (2017). Subretinal injection: A review on the novel route of therapeutic delivery for vitreoretinal diseases. Ophthalmic Res. *58*, 217–226.

57. Penn, J.S., Madan, A., Caldwell, R.B., Bartoli, M., Caldwell, R.W., and Hartnett, M.E. (2008). Vascular endothelial growth factor in eye disease. Prog. Retin. Eye Res. *27*, 331–371.

58. Kwak, N., Okamoto, N., Wood, J.M., and Campochiaro, P.A. (2000). VEGF is major stimulator in model of choroidal neovascularization. Invest. Ophthalmol. Vis. Sci. *41*, 3158–3164.

59. Krzystolik, M.G., Afshari, M.A., Adamis, A.P., Gaudreault, J., Gragoudas, E.S., Michaud, N.A., Li, W., Connolly, E., O'Neill, C.A., and Miller, J.W. (2002). Prevention of experimental choroidal neovascularization with intravitreal anti-vascular endothelial growth factor antibody fragment. Arch. Ophthalmol. *120*, 338–346.

60. Kim, S.J., Toma, H.S., Barnett, J.M., and Penn, J.S. (2010). Ketorolac inhibits choroidal neovascularization by suppression of retinal VEGF. Exp. Eye Res. *91*, 537–543.

61. Bae, J.H., Hwang, A.R., Kim, C.Y., Yu, H.G., Koh, H.J., Yang, W.I., Chang, H.R., and Lee, S.C. (2017). Intravitreal itraconazole inhibits laser-induced choroidal neovascularization in rats. PLoS ONE *12*, e0180482.

62. Yi, X., Ogata, N., Komada, M., Yamamoto, C., Takahashi, K., Omori, K., and Uyama, M. (1997). Vascular endothelial growth factor expression in choroidal neovascularization in rats. Graefes Arch. Clin. Exp. Ophthalmol. *235*, 313–319.

63. Ishibashi, T., Hata, Y., Yoshikawa, H., Nakagawa, K., Sueishi, K., and Inomata, H. (1997). Expression of vascular endothelial growth factor in experimental choroidal neovascularization. Graefes Arch. Clin. Exp. Ophthalmol. *235*, 159–167.

64. Wada, M., Ogata, N., Otsuji, T., and Uyama, M. (1999). Expression of vascular endothelial growth factor and its receptor (KDR/flk-1) mRNA in experimental choroidal neovascularization. Curr. Eye Res. *18*, 203–213.

65. Heier, J.S., Antoszyk, A.N., Pavan, P.R., Leff, S.R., Rosenfeld, P.J., Ciulla, T.A., Dreyer, R.F., Gentile, R.C., Sy, J.P., Hantsbarger, G., and Shams, N. (2006). Ranibizumab for treatment of neovascular age-related macular degeneration: a phase I/II multicenter, controlled, multidose study. Ophthalmology *113*, 633.e1–633.e4.

66. Saishin, Y., Saishin, Y., Takahashi, K., Lima e Silva, R., Hylton, D., Rudge, J.S., Wiegand, S.J., and Campochiaro, P.A. (2003). VEGF-TRAP(R1R2) suppresses choroidal neovascularization and VEGF-induced breakdown of the blood-retinal barrier. J. Cell. Physiol. *195*, 241–248.

67. Eichler, W., Reiche, A., Yafai, Y., Lange, J., and Wiedemann, P. (2008). Growth-related effects of oxidant-induced stress on cultured RPE and choroidal endothelial cells. Exp. Eye Res. *87*, 342–348.

68. Farjood, F., and Vargis, E. (2017). Physical disruption of cell-cell contact induces VEGF expression in RPE cells. Mol. Vis. *23*, 431–446.

69. Hornig, C., Barleon, B., Ahmad, S., Vuorela, P., Ahmed, A., and Weich, H.A. (2000). Release and complex formation of soluble VEGFR-1 from endothelial cells and biological fluids. Lab. Invest. *80*, 443–454.

70. Rajakumar, A., Powers, R.W., Hubel, C.A., Shibata, E., von Versen-Höynck, F., Plymire, D., and Jeyabalan, A. (2009). Novel soluble Flt-1 isoforms in plasma and cultured placental explants from normotensive pregnant and preeclamptic women. Placenta *30*, 25–34.

71. You, Q.S., Gaber, R., Meshi, A., Ramkumar, H.L., Alam, M., Muftuoglu, I.K., and Freeman, W.R. (2018). High-dose high-frequency aflibercept for recalcitrant neovascular age-related macular degeneration. Retina *38*, 1156–1165.

72. Lu, F., and Adelman, R.A. (2009). Are intravitreal bevacizumab and ranibizumab effective in a rat model of choroidal neovascularization? Graefes Arch. Clin. Exp. Ophthalmol. *247*, 171–177.

73. Cao, J., Murat, C., An, W., Yao, X., Lee, J., Santulli-Marotto, S., Harris, I.R., and Inana, G. (2016). Human umbilical tissue-derived cells rescue retinal pigment epithelium dysfunction in retinal degeneration. Stem Cells *34*, 367–379.

74. Bora, P.S., Kaliappan, S., Xu, Q., Kumar, S., Wang, Y., Kaplan, H.J., and Bora, N.S. (2006). Alcohol linked to enhanced angiogenesis in rat model of choroidal neovascularization. FEBS J. *273*, 1403–1414.